

Influence of El Niño Southern Oscillation on global hydropower production

This content has been downloaded from IOPscience. Please scroll down to see the full text.

2017 Environ. Res. Lett. 12 034010

(<http://iopscience.iop.org/1748-9326/12/3/034010>)

View [the table of contents for this issue](#), or go to the [journal homepage](#) for more

Download details:

IP Address: 210.77.64.106

This content was downloaded on 30/03/2017 at 11:28

Please note that [terms and conditions apply](#).

You may also be interested in:

[Hydropower versus irrigation—an analysis of global patterns](#)

Ruijie Zeng, Ximing Cai, Claudia Ringler et al.

[The role of storage capacity in coping with intra- and inter-annual water variability in large river basins](#)

Franziska Gaupp, Jim Hall and Simon Dadson

[Benchmarking carbon fluxes of the ISIMIP2a biome models](#)

Jinfeng Chang, Philippe Ciais, Xuhui Wang et al.

[Towards a global water scarcity risk assessment framework: incorporation of probability distributions and hydro-climatic variability](#)

T I E Veldkamp, Y Wada, J C J H Aerts et al.

[Sustainability of global water use: past reconstruction and future projections](#)

Yoshihide Wada and Marc F P Bierkens

[Impacts of recent drought and warm years on water resources and electricity supply worldwide](#)

Michelle T H van Vliet, Justin Sheffield, David Wiberg et al.

[Large storage operations under climate change: expanding uncertainties and evolving tradeoffs](#)

Matteo Giuliani, Daniela Anghileri, Andrea Castelletti et al.

[Comment on 'An index-based framework for assessing patterns and trends in river fragmentation and flow regulation by global dams at multiple scales'](#)

Thomas Hennig and Darrin Magee

Environmental Research Letters



LETTER

Influence of El Niño Southern Oscillation on global hydropower production

OPEN ACCESS

RECEIVED

13 September 2016

REVISED

1 February 2017

ACCEPTED FOR PUBLICATION

7 February 2017

PUBLISHED

2 March 2017

Original content from this work may be used under the terms of the [Creative Commons Attribution 3.0 licence](#).

Any further distribution of this work must maintain attribution to the author(s) and the title of the work, journal citation and DOI.



Jia Yi Ng^{1,2,4}, Sean W D Turner¹ and Stefano Galelli³

¹ SUTD-MIT International Design Centre, 8 Somapah Rd, Singapore 487372, Singapore

² Veolia City Modelling Centre, Cleantech Park, Singapore 637141, Singapore

³ Pillar of Eng. Systems and Design, Singapore Univ. of Tech. and Design, 8 Somapah Rd, Singapore 487372, Singapore

⁴ Author to whom any correspondence should be addressed.

E-mail: jiayi_ng@mymail.sutd.edu.sg

Keywords: hydropower, El Niño Southern Oscillation, climate variability, global scale, water-energy nexus

Supplementary material for this article is available [online](#)

Abstract

El Niño Southern Oscillation (ENSO) strongly influences the global climate system, affecting hydrology in many of the world's river basins. This raises the prospect of ENSO-driven variability in global and regional hydroelectric power generation. Here we study these effects by generating time series of power production for 1593 hydropower dams, which collectively represent more than half of the world's existing installed hydropower capacity. The time series are generated by forcing a detailed dam model with monthly-resolution, 20th century inflows—the model includes plant specifications, storage dynamics and realistic operating schemes, and runs irrespectively of the dam construction year. More than one third of simulated dams exhibit statistically significant annual energy production anomalies in at least one of the two ENSO phases of El Niño and La Niña. For most dams, the variability of relative anomalies in power production tends to be less than that of the forcing inflows—a consequence of dam design specifications, namely maximum turbine release rate and reservoir storage, which allows inflows to accumulate for power generation in subsequent dry years. Production is affected most prominently in Northwest United States, South America, Central America, the Iberian Peninsula, Southeast Asia and Southeast Australia. When aggregated globally, positive and negative energy production anomalies effectively cancel each other out, resulting in a weak and statistically insignificant net global anomaly for both ENSO phases.

1. Introduction

El Niño Southern Oscillation (ENSO) is a major driver of global interannual climate variability (McPhaden *et al* 2006). Its characteristic warming (El Niño) and cooling (La Niña) phases manifest in flood and drought conditions across many regions of the world (Chiew and McMahon 1998, Yu and Zou 2013, Ward *et al* 2014, Liang *et al* 2016). This raises the prospect of ENSO-driven variability in hydroelectric power production at dams located in affected river basins. A link between ENSO and global hydropower production would carry important practical implications. For example, it has been speculated that volatility in hydropower production could be influencing global carbon emissions and fossil fuel prices—

a result of periodic hydropower production shortfalls being offset by increased energy production from coal, oil and gas fired plants (Cashin *et al* 2015). Hydropower is the dominant source of electrical power production in many world regions (~17% globally) and new dam developments are expected to both secure and extend its role in future (Hertwich *et al* 2015, IEA 2015, EIA 2016). A study into the potential relationship between ENSO and global and regional hydropower production would therefore constitute a highly relevant and timely contribution to the water-energy nexus agenda (see Frumhoff *et al* 2015).

The most intuitive approach to studying the relationship between ENSO and hydropower production would be to look for correlations between

historically measured ENSO indices and records of electricity production from hydropower plants. Unfortunately, the available electricity production records are both short and coarse (thirty years' country-level records of annual energy production—EIA 2016), posing at least three problems for such an analysis. First, the short period of record encompasses only a handful of El Niño events, limiting the prospects for finding robust, ENSO-driven anomalies in energy production. Second, country-level data may mask important differences in ENSO impact across different dams within large countries, like China or the United States. Third, many large hydropower dams have come online in recent years and are therefore unrepresented in historical hydropower production data. A practical approach that overcomes these issues is simulation, which can be used to generate synthetic hydropower production data for individual dams—including those built only recently—under the ENSO events experienced during the bulk of the 20th century. The key challenge with this approach is to represent adequately the actual water release schemes used by dam operators—an issue that has been addressed in prior large scale water resources studies using heuristics or optimized operations tailored to the reservoir function (Lehner *et al* 2005, Haddeland *et al* 2006, Hanasaki *et al* 2006, Hamududu and Killingtveit 2012, van Vliet *et al* 2016).

Here we quantify the potential impacts of ENSO on global and regional hydropower production by simulating 1593 hydropower dams—representing more than half the world's currently installed hydropower capacity. Each dam is assigned a bespoke, optimized operating policy and then forced with monthly-resolution inflows derived from 20th century climate conditions. Monthly time series of hydropower production are calculated accounting for reservoir storage dynamics and coinciding changes to hydraulic head as well as evaporation losses from the water surface. Our approach allows us to explore fine-detail temporal and spatial patterns of global hydropower production, and link these patterns to all ENSO episodes observed during the period 1906–2000.

2. Methods

To undertake this analysis, we compile data describing the design specifications of existing hydropower dams. Next, we obtain inflow time series for all dams using gridded historical climate data and a global hydrological model. We assign each dam a bespoke, optimized operating policy to provide a realistic basis for water release decisions that affect hydropower production. We then simulate each dam to produce time series of hydropower production, which are analyzed to identify anomalies in power production during El Niño and La Niña phases. These steps are detailed in the following subsections, and the overall approach is validated using records of annual hydropower

production for each country (see supplementary data available at stacks.iop.org/ERL/12/034010/mmedia).

2.1. Data for hydropower dams

Design specifications of 1593 hydropower dams, including dam height, maximum reservoir surface area, storage capacity, latitude, longitude, upstream catchment area, and long-term average inflow, are obtained from the Global Reservoir and Dam (GRanD) database (Lehner *et al* 2011). These properties are cross-checked and, where necessary, infilled using other sources, specifically the International Commission on Large Dams (ICOLD 2011) and Global Lakes and Wetlands Database (Lehner and Döll 2004). We include run-of-river hydropower dams, but exclude pumped-storage reservoirs, for which suitable inflow data are unavailable. Installed power capacities are obtained from the ICOLD and Global Energy Observatory (GEO 2016) databases. The maximum flow rate through turbines is provided by GEO for about 15% of the reservoirs. For the remaining reservoirs, the maximum turbine flow rate is predicted through a regression model using the installed capacity and long-term average discharge as predictors ($R^2 = 0.749$).

To define an archetypal reservoir shape, we implement Kaveh's method (Kaveh *et al* 2013). The reservoir surface area, a , is equal to $A_m \times (v/V_m)^{(2-N)/2}$, where v is volume of water in storage, A_m , V_m and y_m are maximum surface area, volume and depth respectively, and N is a unique reservoir coefficient defined as $2 \times V_m/(y_m \times A_m)$. Maximum depth is taken as two meters less than dam height to allow for freeboard. For the small number of instances in which the maximum depth is not available, we adopt Liebe's method, which assumes that the reservoir is shaped like a top-down pyramid cut diagonally in half (Liebe *et al* 2005). Active (usable) storage capacity is not available from the GRanD database and is assumed to equal to storage capacity unless available through GEO.

2.2. Hydrological model

We develop for each dam a historical monthly inflow time series using the $0.5^\circ \times 0.5^\circ$ gridded global runoff data set provided by the Water and Global Change (WATCH) 20th Century (1906–2000) Model Output (Weedon *et al* 2011). The runoff data are generated by forcing a global hydrological model, named WaterGAP (Alcamo *et al* 2003), which computes accumulated runoff for each grid square using the DDM30 river network (Döll and Lehner 2002). WaterGAP is calibrated with discharge data provided by the Global Runoff Data Center (GRDC 1999). Overall, the model performance is reasonable, although runoff may be underestimated in snow-dominated areas and overestimated in semiarid or arid regions (Döll *et al* 2003). Nevertheless, WaterGAP has been applied successfully in various global and continental water resources studies (e.g. Lehner *et al* 2005, Naidoo *et al* 2008, Döll

Table 1. Years categorized as El Niño and La Niña.

ENSO phase	Hydrological year
El Niño	1912, 1914, 1919, 1926, 1930, 1931, 1941, 1952, 1958, 1964, 1966, 1970, 1973, 1977, 1983, 1987, 1988, 1992, 1998
La Niña	1907, 1909, 1910, 1911, 1917, 1923, 1925, 1939, 1943, 1945, 1950, 1955, 1956, 1957, 1965, 1968, 1971, 1972, 1974, 1975, 1976, 1989, 1999, 2000

Source: coaps.fsu.edu/jma.shtml.

et al 2009, Haddeland *et al 2014*, Veldkamp *et al 2015*). Here we implement an additional minor correction to the discharge to adjust for any disparity between upstream catchment area defined by the DDM30 river network and the documented upstream catchment area of each dam.

2.3. Dam operating model

To simulate the behavior of the hydropower dam operators, we model the decision-making problem faced by the human regulators as an optimal control problem, whose objective is to maximize hydropower production over the long term. The problem is solved using Stochastic Dynamic Programming. The chosen approach uses the reservoir specifications and a periodic Markov chain model of the inflow process to generate a bespoke look-up table of turbine release decisions for each dam. Releases are specified as a function of month of the year, storage level, and current period inflow—common choices for state variables in actual dam operation (Hejazi *et al 2008*). We simulate each dam using these operating rules to produce realistic hydropower generation time series under 1906–2000 climate conditions. To account for the long term signal related to the expansion of hydropower capacity during the past decades, we simulate all dams from 1906 onwards regardless of their construction year. In other words, we simulate the behavior of existing dams under the 20th century inflow conditions, which serve as representation of climate variability (although dam construction year is accounted for in model validation, which compares simulated to observed generation).

Storage dynamics are simulated using the laws of mass balance:

$$\begin{aligned} S_{t+1} &= S_t + Q_t - R_t - E_t \\ 0 &\leq S_t \leq S_{\text{cap}} \\ 0 &\leq R_t \leq \min(S_t + Q_t - E_t, R_{\text{max}}) \end{aligned} \quad (1)$$

where S_t is the reservoir storage, Q_t is the current period reservoir inflow volume, E_t is the evaporation loss and R_t is the water release volume recommended by the operating rules at time t . S_{cap} is the capacity of the reservoir and R_{max} is the maximum volume of water that can be released through the turbines during any month of operations (computed from maximum turbine release rate). Release decisions must also satisfy downstream environmental flow requirements. These allocations are determined using the variable monthly flow method: each month is categorized as low-flow (mean monthly flow <40% mean annual

flow), intermediate flow (40%–80%) or high flow (>80%) and then allocated a release requirement equal to 60, 45 and 30% for the respective categories (Pastor *et al 2014*). All excess water is spilled (spilled volume at time t is equal to $S_t + Q_t - R_t - E_t - S_{\text{cap}}$). Evaporation is a function of the average storage between t and $t + 1$, creating an equation with two unknowns (E_t and S_{t+1}) that is solved by iteration at each step of the simulation.

Hydropower production P_t (MW) is calculated as follows:

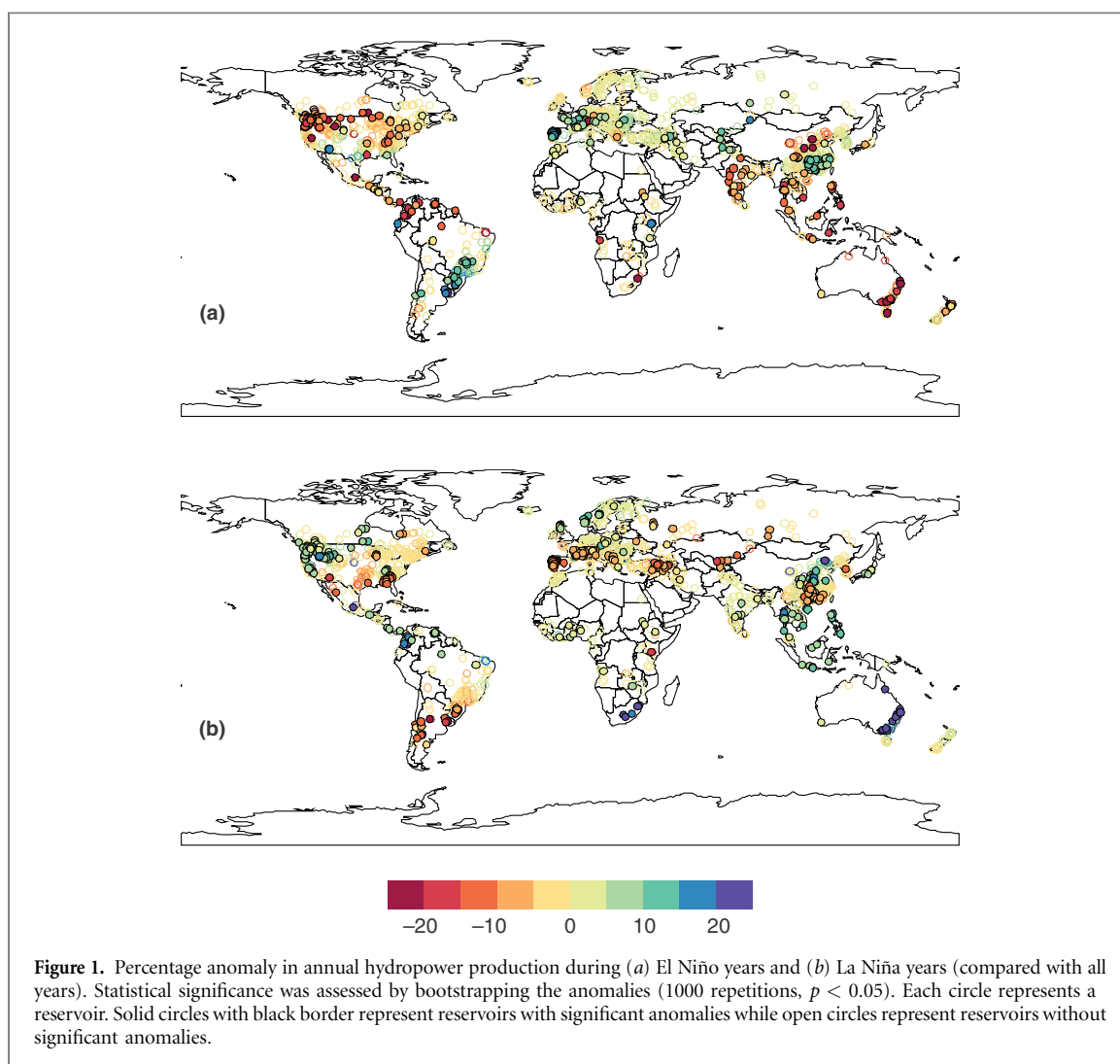
$$P_t = \eta \times \rho \times g \times r_t \times H_t \quad (2)$$

where η is turbine efficiency, ρ is the water density (1000 kg m^{-3}), g is gravitational acceleration (m s^{-2}), H_t is hydraulic head (m) (taken as the average between t and $t + 1$), and r_t is the average release rate ($\text{m}^{-3} \text{ s}^{-1}$) implied by monthly release volume R_t . Maximum hydraulic head is calculated by assuming turbine efficiency equal to 0.9. In cases where both maximum turbine flow and maximum hydraulic head are available, the efficiency of hydropower reservoir is computed, ensuring that equation (2) holds true for all reservoirs operating under maximum capacity. All optimization and simulation algorithms are implemented using R package *reservoir* (Turner and Galelli 2016).

2.4. Statistical analysis

To analyze the potential impact of ENSO on simulated hydropower production, we look for statistically significant anomalies in production occurring during recognized ENSO phases (i.e. El Niño and La Niña years). We begin by aggregating the monthly hydropower production of each dam into annual time series based on hydrological years (1907 to 2000). Hydrological years are referred to by the year in which they end (e.g. hydrological year 1907 refers to the period October 1906–September 1907). El Niño and La Niña years are identified using the Center for Ocean-Atmospheric Prediction Studies classification shown in table 1 (ENSO years are referred to by the year in which they start, so they are adjusted in table 1 to match the definition of hydrological years). We calculate the ENSO year percentage anomalies in hydropower production for each dam compared to all years. Statistical significance is assessed by bootstrapping the anomalies for 1000 repetitions.

We also examine correlations between simulated annual power production and the extended Multivariate ENSO Index (MEI) derived from sea-level



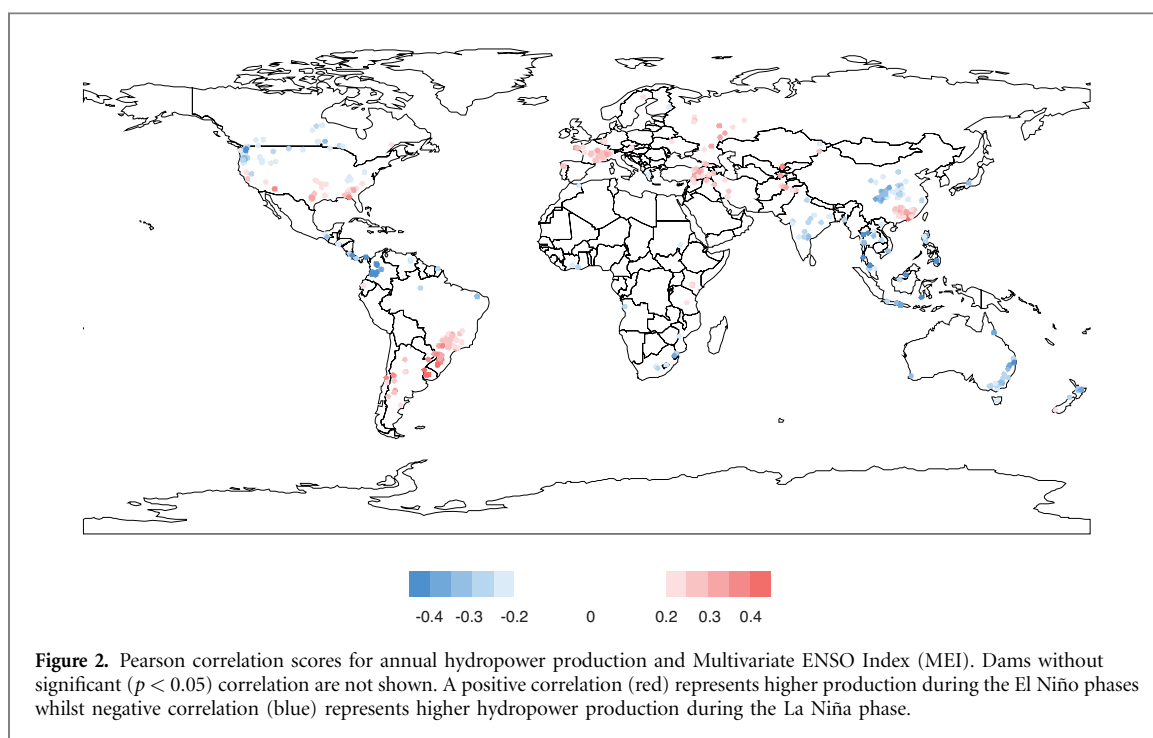
pressure and sea surface temperature over the tropical Pacific. The MEI is available from the Earth System Research Laboratory (ESRL 2016) and is used commonly to indicate the presence of ENSO phases.

To assess absolute production anomalies aggregated for countries, regions, and at the global level, we need to account for dams not represented in the simulations. We extrapolate to total global production using the ratio of simulated to actual capacity for each country, as in van Vliet *et al* (2016). Actual installed capacities for each country are the 2012 values obtained from the US Energy Information Administration (EIA 2016). We then aggregate to analyze ENSO impacts on hydropower production at regional and global scales.

3. Results

We find statistically significant anomalies in annual hydropower production ($p < 0.05$) for 34.7% of simulated dams during at least one of the two ENSO phases of El Niño and La Niña (figure 1). El Niño and La Niña phases cause a statistically significant anomaly in 22% and 24% of dams respectively (or 26% and

28% of global installed capacity). In both El Niño and La Niña phases, the number of dams showing significant positive anomalies is almost identical to the number of dams showing significant negative anomalies—indicating a possible balancing effect occurring during each ENSO phase. Affected dams are located predominantly within the northwestern parts of the United States, Central America, Iberian Peninsula, South China, Southeast Asia and Australia. Europe (excluding the Iberian Peninsula) is a relatively weakly affected region. This is unsurprising since climate variability in Europe is driven mainly by hydroclimatic phenomena unrelated to ENSO (Rogers 1997). Yet—in agreement with recent studies (e.g. Capa-Morocho *et al* 2014)—some significant anomalies are detected during the El Niño phase, indicating that ENSO may have weak influence in Europe. Globally, only 11% of dams show significant anomalies during both El Niño and La Niña years, meaning many dams are significantly impacted by only one of the two ENSO phases. For instance, hydropower production in the Indian subcontinent is substantially reduced during El Niño events, yet is barely affected during La Niña—a consequence of the weakening of the Indian Monsoon during El Niño episodes (Kumar



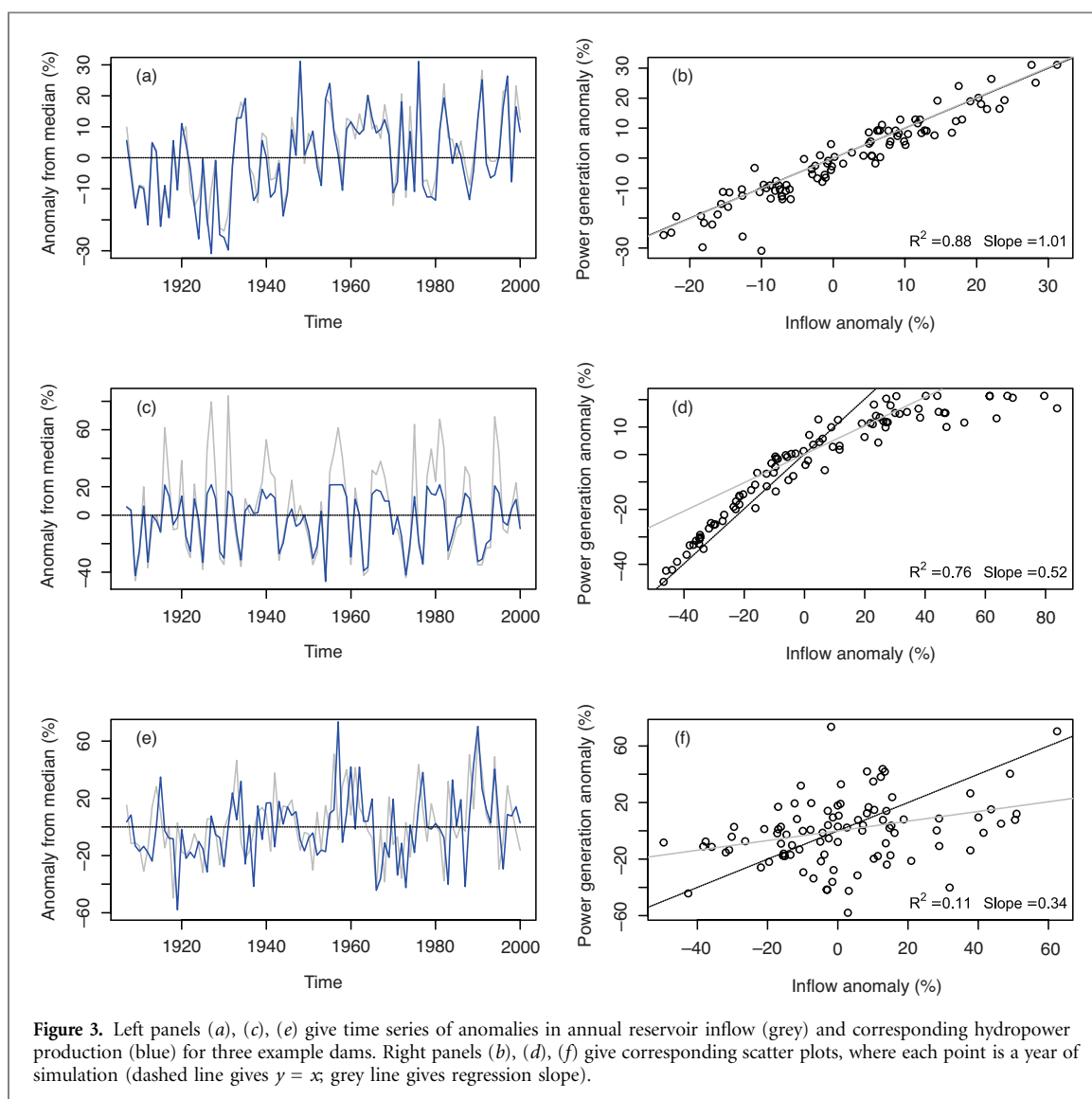
et al 2006). Other instances include the southeastern edge of South America and western Asia.

Figure 2 displays Pearson correlation scores for simulated annual hydropower production with the extended Multivariate ENSO Index. Hydropower production correlates significantly ($p < 0.05$) with MEI for 27.4% of reservoirs—close to the 34.7% of reservoirs exhibiting significant hydropower production anomalies in at least one ENSO phase. The world regions featuring significant correlations generally correspond to those showing a strong teleconnection between ENSO indices and precipitation (or streamflow) patterns, as identified in several prior global and regional studies (e.g. Ropelewski and Halpert 1986, Chiew and McMahon 1998, Grimm *et al* 2000, Kumar *et al* 2006, Räsänen and Kumm 2013).

Anomalies in annual reservoir inflow totals (as measured by percentage deviation from median) tend to correlate strongly with corresponding anomalies in hydropower production (R^2 exceeds 0.9, 0.8, 0.7 and 0.6 in 28, 47, 62 and 71% of dams respectively). Power production anomalies often track inflow anomalies closely throughout the simulation period ($\sim 26\%$ dams exhibit regression slope in the range 0.9–1.1), as exemplified in figure 3(a). In other cases we find that the power generation signal is dampened relative to the inflow—a phenomenon largely attributable to dam design specifications. Figure 3(c) highlights this behavior. The dam appears to be unable to fully convert large inflow volumes into power, which would occur if the reservoir is full (meaning excess inflows are spilled) or if inflow exceeds maximum turbine release rates. The latter results in accumulation of inflows in storage, which explains why negative inflow anomalies are blunted in the power anomaly series for this particular dam and for many others (inflows can be

accumulated in storage and released to generate power during future dry years). Indeed, the regression slope, which indicates the extent of smoothing (figure 3(d)), can be explained by the factors relating to maximum turbine release rate (e.g. maximum turbine release rate as a percentage of mean inflow, giving a ranked correlation score of 0.7) as well as the coefficient of variation in monthly and annual inflows (greater variability leads to greater likelihood of breaching maximum release rates). Some dams exhibit a near complete breakdown between annual inflow and power generation anomalies ($\sim 16\%$ dams with R^2 less than 0.4). As figure 3(e) shows, positive power generation anomalies can lag a year or two behind positive inflow anomalies. Reservoirs that fill quickly (low capacity relative to mean inflow) and empty slowly (high capacity relative to maximum release rate) are common in this category, suggesting the role of storage accumulation during high inflow years, leading to high hydraulic head. Often these accumulations will be a direct consequence of operator behavior (i.e. gathering water to raise production with a higher hydraulic head to maximize long term revenues). The presence of these behaviors highlights the importance of simulating hydropower production with a model of the dam and its operations, as opposed to inferring production with a statistical model fed by the inflow time series.

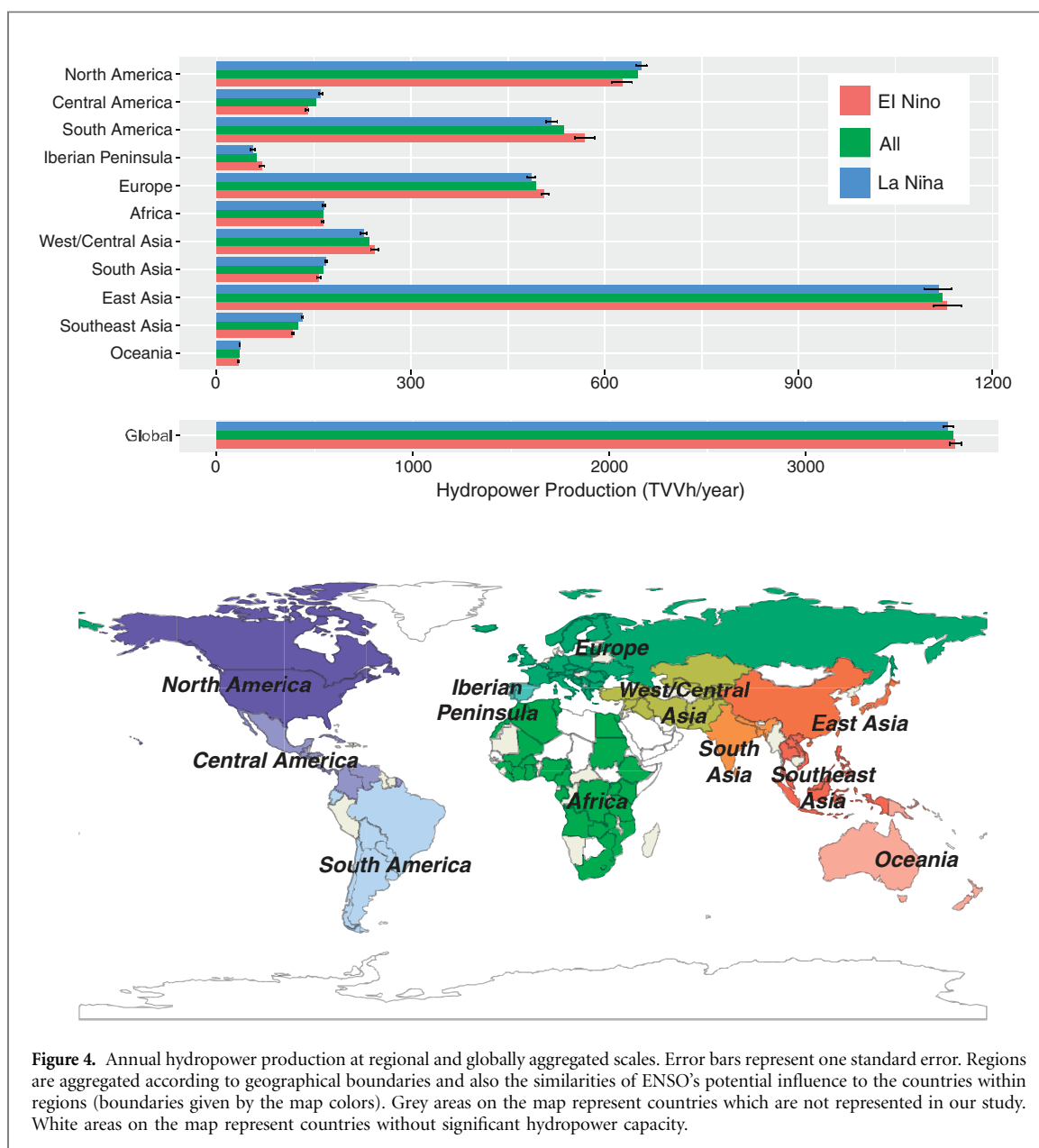
Regionally aggregated hydropower production anomalies reveal statistically significant change in hydropower production in six out of eleven regions during at least one ENSO phase ($p < 0.05$) (figure 4). Southeast Asia, Central America, and Iberian Peninsula experience the largest relative excursions in net hydropower production (percentage anomaly of at least 4.7%) during both ENSO phases. China has



the world's largest installed hydropower capacity and dominates the aggregated impact on production in East Asia. So whilst hydropower production anomalies in East Asia are small in relative terms, the absolute impact during El Niño years is surpassed only by American regions. Figure 5 displays regionally aggregated simulation results as annual time series of percentage production anomalies. Results show that in some regions, particularly Southeast Asia, South Asia and Central America, the hydropower production anomalies are tightly phased with El Niño and La Niña years. The largest deviations from the long-term mean generally correspond to strong ENSO events. Production variability across different episodes of a given ENSO phase may also be due to the non-stationarity of ENSO influence caused by interdecadal modulation of ENSO teleconnections (Gershunov and Barnett 1998, Power *et al* 1999, Wang *et al* 2008, Feng *et al* 2014). Other regions show pronounced percentage hydropower production anomalies during ENSO phases as well as neutral years. The Iberian Peninsula, for instance, exhibits an average 11% change in

hydropower production during both ENSO phases; yet the variance of the anomalies across the different El Niño episodes results in an insignificant aggregated anomaly for El Niño years (at $p = 0.10$).

When anomalies are aggregated globally, we detect no significant net impact of either ENSO phase on hydropower production (figure 4, figure 5). Annual global hydropower production is on average 0.35% higher during El Niño years and 0.64% lower during La Niña years as compared to all years—differences which are not significant at $p = 0.10$. In other words, regional differences in hydropower production appear to balance each other out almost perfectly. The weak residual signal in net global production resulting from either ENSO phase is eclipsed by production anomalies driven by other sources of interannual variability. This balancing is also observed within some regions, notably Africa, where the impact of ENSO on dams in East Africa is balanced by impacts experienced on the remainder of the continent, and East Asia, where the impacts in northern China balance impacts in southern China. The results thereby demonstrate that weak anomalies in power production at global

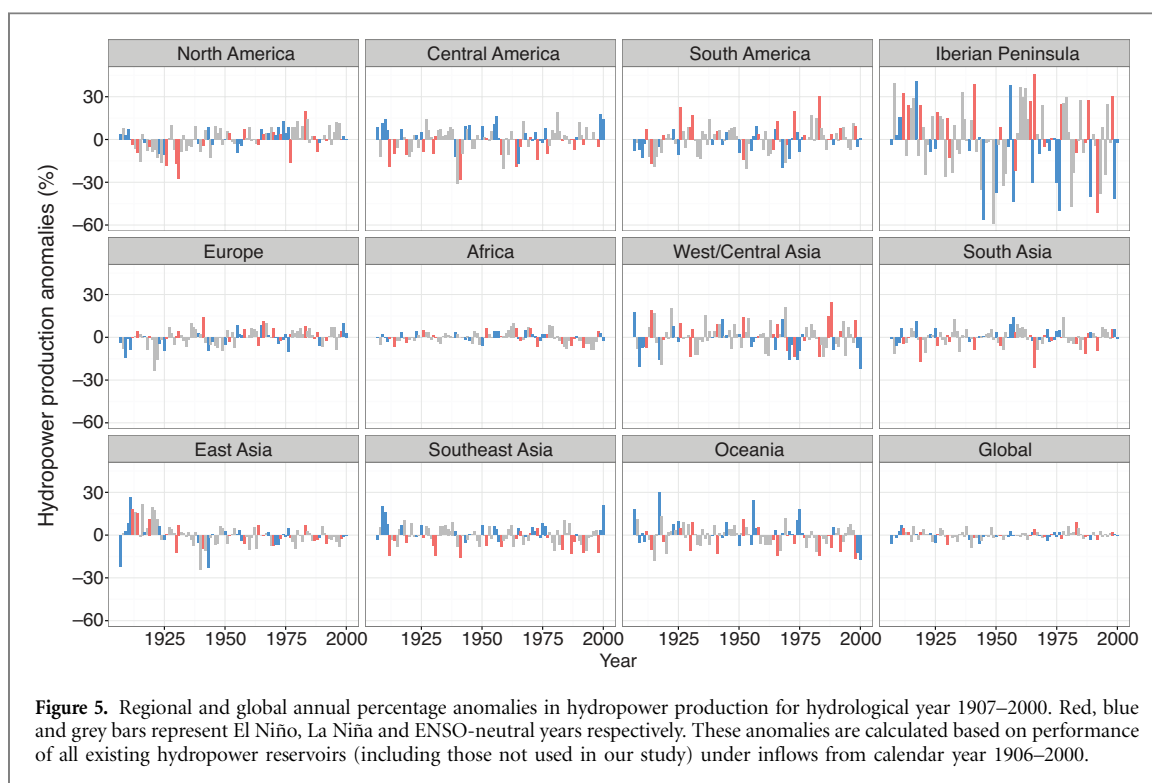


and continental scales may mask important anomalies at subcontinental scales.

4. Discussion

The analysis reported above highlights the importance of detailed dam models in global hydropower studies involving simulation. The variability in power generation resulting from inflow variability is largely a function of reservoir specifications, namely maximum turbine rates, storage and operator decision making. These need to be captured to model a power production time series correctly. We also find that relatively low anomalies in power production at large spatial scales potentially mask important anomalies for individual regions, countries, river basins or dams. Furthermore, El Niño and La Niña phases can affect production in markedly different ways, as seen in India, South America and West Asia, meaning each

phase must be isolated and studied separately. Yet, our approach based on simulated hydropower production has some limitations. First, the dam model assumes that the operator wants to maximize hydropower production, which may inaccurately represent the operations of dams that contribute stable power supply or serve other purposes (e.g. irrigation, flood control). Second, reliance on reanalysis climate data from WATCH and downscaling from 0.5° grids may also result in incorrect inflows for dams in parts of the world where there are sharp changes in rainfall and runoff over short distances. Third, extrapolation to regional and global production assumes that unrepresented reservoirs have similar performance and spatial distribution as those modeled reservoirs. These limitations may result in a poor fit between modeled and observed hydropower production for countries like Brazil and Australia, but regions experiencing the highest anomalies, namely Central American, Iberian



Peninsula and Southeast Asia, are modeled well (see supplementary data).

The significant, ENSO-driven, subcontinental hydropower production anomalies that we observe may carry broad practical implications at regional and global scale. Shortfalls in hydropower production must result in either reduced available electrical energy for consumers or, more likely, a temporary shift in the means of power generation. Net exporters of hydroelectric power will lose revenues whilst net importers will need to augment supplies from alternative resources, including coal, oil and gas fired plants. Regional carbon emissions and fossil fuel prices may be impacted by hydropower shortfall in this way (Cashin *et al* 2015)—as observed recently during dry spells in California (Gleick 2015) and Tanzania (World Bank 2004). The opposite is also plausible; heavy rains in the arid west of the United States connected to the 1997–1998 El Niño event are thought to have contributed to increased hydropower output, leading to reduced energy costs (Changnon 1999). Although regional impact may be relatively small, the cumulative impact can be staggering (Hardin *et al* 2017), especially when multiple regions are affected by ENSO simultaneously. The scale of these impacts is likely to depend on both the magnitude of the hydropower production shortfall and the relative importance of hydropower in regional energy supplies. Complimentary future research on the role of ENSO in controlling other means of power generation (e.g. water availability for thermal plant power generation) will help define global vulnerability hotspots where energy supplies are critically exposed to interannual climate variability.

It is also interesting to consider whether planned developments have the potential to create vulnerabilities in regional supply networks by increasing reliance on hydroelectric power supplies, thereby exposing them to ENSO variability. The Mekong River is one example. It remains one of the world's few large rivers that has yet to be heavily exploited for its hydropower potential, and at least eleven dam projects are planned for the middle and lower reaches of the river basin (Winemiller *et al* 2016). We expect that developments within the upstream mountainous regions of Tibet and Yunnan provinces would be relatively unaffected by ENSO. But downstream projects in Laos and Cambodia, as well as on the Salween River in Myanmar and Thailand, all lie within regions that we would expect to experience significant reductions in power production during the El Niño phase (Räsänen and Kummu 2013). These reductions may be exacerbated in the coming decades by the expected intensification of El Niño-driven drying in the west Pacific (Power *et al* 2013). Another example is the hydropower development in the Amazon region. We would expect new dams in the Amazon to experience significant reductions in power generation during El Niño—this may provide an opportunity for transmission of power via the National Interconnected System in Brazil (da Silva and Freitas 2011), which appears to experience opposing signals of power production in the north and south during ENSO events. Impacts on other regions with ongoing hydropower developments, such as the Congo basin, are less predictable given the lack of reservoir data. Overall, examples like this emphasize the need for regional energy investment strategies that allow for the

possibility of significant, periodic down-shifts in regional hydropower production. The issue gains prominence in light of evidence suggesting that strong ENSO events will occur more frequently in future under greenhouse warming (Cai *et al* 2014).

5. Conclusion

Our study quantifies the impact of the 20th century ENSO episodes on global and regional hydropower production. 1593 hydropower dams are simulated using a detailed dam model forced with inflows from 1906–2000 (regardless of the construction year of the dam). Results show that regions characterized by a strong teleconnection between ENSO indices and streamflow patterns are likely to exhibit hydropower anomalies—as confirmed by the 27.4% of simulated dams showing statistically significant correlation between the Multivariate ENSO Index and hydropower production. Interestingly, some dams within the regions influenced by ENSO may not exhibit hydropower anomalies due to their design specifications and operator decision-making. These results extend our current understanding of ENSO impact on global hydrology and highlight the potential effect of climate variability on the water-energy nexus. Our results may be used in conjunction with regional-scale studies on water-energy nexus, which often lack suitable time series data for hydropower production (Conway *et al* 2015). A similar modeling approach—with non-static operating rules to account for climatic adaption (Rheinheimer and Viers 2015, Rheinheimer *et al* 2016)—could be applied to future runoff series obtained from climate change scenarios. Such a study would inform decision makers of necessary investments needed for capital-intensive hydropower dams to ensure regional energy security in the face of climate change.

Acknowledgments

The material reported in this document is supported by the SUTD-MIT International Design Centre (IDC)—research grant IDG 21400101. Any findings, conclusions, recommendations, or opinions expressed in this document are those of the authors and do not necessarily reflect the views of the IDC. We would like to thank Karen Willcox for her valuable comments on our research.

References

- Alcamo J, Döll P, Henrichs T, Kaspar F, Lehner B, Röscher T and Siebert S 2003 Development and testing of the WaterGAP 2 global model of water use and availability *Hydrol. Sci. J.* **48** 317–37
- Cai W *et al* 2014 Increasing frequency of extreme El Niño events due to greenhouse warming *Nat. Clim. Change* **4** 111–16
- Capa-Morocho M, Rodríguez-Fonseca B and Ruiz-Ramos M 2014 Crop yield as a bioclimatic index of El Niño impact in Europe: Crop forecast implications *Agr. Forest Meteorol.* **198** 42–52
- Cashin P A, Mohaddes K and Raissi M 2015 Fair weather or foul? The macroeconomic effects of El Niño *Social Science Research Network* (<https://doi.org/10.2139/ssrn.2643965>)
- Changnon S A 1999 Impacts of 1997–98 El Niño-generated weather in the United States *Bull. Am. Meteorol. Soc.* **80** 1819–27
- Chiew F H and McMahon T A 1998 Global ENSO—streamflow teleconnection, streamflow forecasting and interannual variability *Hydrol. Sci.* **47** 505–22
- Conway D *et al* 2015 Climate and southern Africa's water-energy-food nexus *Nat. Clim. Change* **5** 837–46
- da Silva Soito J L and Freitas M A V 2011 Amazon and the expansion of hydropower in Brazil: Vulnerability, impacts and possibilities for adaptation to global climate change *Renew. Sust. Energ. Rev.* **15** 3165–77
- Döll P and Lehner B 2002 Validation of a new global 30-min drainage direction map *J. Hydrol.* **258** 214–31
- Döll P, Kaspar F and Lehner B 2003 A global hydrological model for deriving water availability indicators: Model tuning and validation *J. Hydrol.* **270** 105–34
- Döll P, Fiedler K and Zhang J 2009 Global-scale analysis of river flow alterations due to water withdrawals and reservoirs *Hydrol. Earth Syst. Sci.* **13** 2413–32
- EIA 2016 International energy statistics (www.eia.gov/)
- ESRL 2016 (www.esrl.noaa.gov/psd/enso/mei.ext/index.html)
- Feng J, Wang L and Chen W 2014 How does the East Asian summer monsoon behave in the decaying phase of El Niño during different PDO phases? *J. Clim.* **27** 2682–98
- Frumhoff P C, Burkett V, Jackson R B, Newmark R, Overpeck J and Webber M 2015 Vulnerabilities and opportunities at the nexus of electricity, water and climate *Environ. Res. Lett.* **10** 080201
- Gershunov A and Barnett T P 1998 Interdecadal modulation of ENSO teleconnections *Bull. Am. Meteorol. Soc.* **79** 2715–25
- Gleick P H 2015 *Impacts of California's ongoing Drought: Hydroelectricity Generation* (Oakland: Pacific Institute)
- Global Energy Observatory 2016 Information on Global Energy Systems and Infrastructure (<http://globalenergyobservatory.org/>)
- GRDC 1999 Observed river discharges, (Global Runoff Data Centre, Koblenz, Germany) *Technical report* (www.bafg.de/GRDC/EN/Home/homepage_node.html)
- Grimm A M, Barros V R and Doyle M E 2000 Climate variability in southern South America associated with El Niño and La Niña events *J. Clim.* **13** 35–58
- Haddeland I, Skaugen T and Lettenmaier D P 2006 Anthropogenic impacts on continental surface water fluxes *Geophys. Res. Lett.* **33** L08406
- Haddeland I *et al* 2014 Global water resources affected by human interventions and climate change *Proc. Natl Acad. Sci. USA* **111** 3251–56
- Hamududu B and Killingtveit A 2012 Assessing climate change impacts on global hydropower *Energies* **5** 305–22
- Hanasaki N, Kanae S and Oki T 2006 A reservoir operation scheme for global river routing models *J. Hydrol.* **327** 22–41
- Hardin E, AghaKouchak A, Qomi M J A, Madani K, Tarroja B, Zhou Y, Yang T and Samuelson S 2017 California drought increases CO₂ footprint of energy *Sustain. Cities Soc.* **28** 450–52
- Hejazi M I, Cai X and Ruddell B L 2008 The role of hydrologic information in reservoir operation—learning from historical releases *Adv. Water Resour.* **31** 1636–50
- Hertwich E G, Gibon T, Bouman E A, Arvesen A, Suh S, Heath G A, Bergesen J D, Ramirez A, Vega M I and Shi L 2015 Integrated life-cycle assessment of electricity-supply scenarios confirms global environmental benefit of low-carbon technologies *Proc. Natl Acad. Sci. USA* **112** 6277–82

- ICOLD 2011 World Register of Dams Version updates 1998–2009 (International Commission on Large Dams, Paris, France) *Technical Report* (www.icold-cigb.net)
- IEA 2015 *World Energy Outlook 2015* (International Energy Agency, Paris, France), *Technical report* (www.worldenergyoutlook.org/weo2015/)
- Kaveh K, Hosseinzadeh H and Hosseini K 2013 A new equation for calculation of reservoir's area-capacity curves *KSCE J. Civ. Eng.* **17** 1149–56
- Kumar K K, Rajagopalan B, Hoerling M, Bates G and Cane M 2006 Unraveling the mystery of Indian monsoon failure during El Niño *Science* **314** 115–19
- Lehner B and Döll P 2004 Development and validation of a global database of lakes, reservoirs and wetlands *J. Hydrol.* **296** 1–22
- Lehner B, Czisch G and Vassolo S 2005 The impact of global change on the hydropower potential of Europe: a model-based analysis *Energ. Policy* **33** 839–55
- Lehner B *et al* 2011 High-resolution mapping of the world's reservoirs and dams for sustainable river-flow management *Front. Ecol. Environ.* **9** 494–502
- Liang Y C, Chou C C, Yu J Y and Lo M H 2016 Mapping the locations of asymmetric and symmetric discharge responses in global rivers to the two types of El Niño *Environ. Res. Lett.* **11** 044012
- Liebe J, van De Giesen N and Andreini M 2005 Estimation of small reservoir storage capacities in a semi-arid environment: A case study in the Upper East Region of Ghana *Phys. Chem. Earth, Parts A/B/C* **30** 448–54
- McPhaden M J, Zebiak S E and Glantz M H 2006 ENSO as an integrating concept in earth science *Science* **314** 1740–45
- Naidoo R, Balmford A, Costanza R, Fisher B, Green R E, Lehner B, Malcolm T R and Ricketts T H 2008 Global mapping of ecosystem services and conservation priorities *Proc. Natl Acad. Sci. USA* **105** 9495–500
- Pastor A V, Ludwig F, Biemans H, Hoff H and Kabat P 2014 Accounting for environmental flow requirements in global water assessments *Hydrol. Earth Syst. Sci.* **18** 5041–59
- Power S, Casey T, Folland C, Colman A and Mehta V 1999 Inter-decadal modulation of the impact of ENSO on Australia *Clim. Dynam.* **15** 319–24
- Power S, Delage F, Chung C, Kociuba G and Keay K 2013 Robust twenty-first-century projections of El Niño and related precipitation variability *Nature* **502** 541–45
- Räsänen T A and Kummu M 2013 Spatiotemporal influences of ENSO on precipitation and flood pulse in the Mekong River Basin *J. Hydrol.* **476** 154–68
- Rheinheimer D E and Viers J H 2015 Combined effects of reservoir operations and climate warming on the flow regime of hydropower bypass reaches of California's Sierra Nevada *River Res. Appl.* **31** 269–79
- Rheinheimer D E, Null S E and Viers J H 2016 Climate-adaptive water year typing for instream flow requirements in California's Sierra Nevada *J. Water Resour. Plan. Manage.* **142** 04016049
- Rogers J C 1997 North Atlantic storm track variability and its association to the North Atlantic Oscillation and climate variability of northern Europe *J. Clim.* **10** 1635–47
- Ropelewski C F and Halpert M S 1986 North American precipitation and temperature patterns associated with the El Niño Southern Oscillation (ENSO) *Mon. Weather Rev.* **114** 2352–62
- Turner S and Galelli S 2016 Water supply sensitivity to climate change: An R package for implementing reservoir storage analysis in global and regional impact studies *Environ. Modell. Softw.* **76** 13–9
- van Vliet M T, Wiberg D, Leduc S and Riahi K 2016 Power-generation system vulnerability and adaptation to changes in climate and water resources *Nat. Clim. Change* **6** 375–80
- Veldkamp T I, Eisner S, Wada Y, Aerts J C and Ward P J 2015 Sensitivity of water scarcity events to ENSO-driven climate variability at the global scale (<http://dare.uvu.vu.nl/handle/1871/53549>)
- Wang L, Chen W and Huang R 2008 Interdecadal modulation of PDO on the impact of ENSO on the East Asian winter monsoon *Geophys. Res. Lett.* **35** L20702
- Ward P J, Jongman B, Kummu M, Dettinger M D, Weiland F C S and Winsemius H C 2014 Strong influence of El Niño Southern Oscillation on flood risk around the world *Proc. Natl Acad. Sci. USA* **111** 15659–64
- Weedon G P, Gomes S, Viterbo P, Shuttleworth W J, Blyth E, Österle H, Adam J C, Bellouin N, Boucher O and Best M 2011 Creation of the WATCH forcing data and its use to assess global and regional reference crop evaporation over land during the twentieth century *J. Hydrometeorol.* **12** 823–48
- Winemiller K *et al* 2016 Balancing hydropower and biodiversity in the Amazon, Congo, and Mekong *Science* **351** 128–29
- World Bank 2004 Technical annex for a proposed credit of SDR 30.2 million (US\$43.8 million equivalent) to the United Republic of Tanzania for an emergency power supply project (African Region Energy Group. World Bank, Washington, DC) *Technical Report* T-7623-T-A (www-wds.worldbank.org/)
- Yu J Y and Zou Y 2013 The enhanced drying effect of Central-Pacific El Niño on US winter *Environ. Res. Lett.* **8** 014019